# Medieval warming initiated exceptionally large wildfire outbreaks in the Rocky Mountains

W. John Calder[a,b,1], Dusty Parker[b], Cody J. Stopka[b], Gonzalo Jiménez-Moreno[c], and Bryan N. Shuman[a,b]

[a]Program in Ecology, University of Wyoming, Laramie, WY 82071; [b]Department of Geology and Geophysics, University of Wyoming, Laramie, WY 82071; and [c]Departamento de Estratigrafía y Paleontología, Universidad de Granada, 18002 Granada, Spain

Edited by Monica G. Turner, University of Wisconsin-Madison, Madison, WI, and approved September 1, 2015 (received for review January 13, 2015)

**Many of the largest wildfires in US history burned in recent decades, and climate change explains much of the increase in area burned. The frequency of extreme wildfire weather will increase with continued warming, but many uncertainties still exist about future fire regimes, including how the risk of large fires will persist as vegetation changes. Past fire-climate relationships provide an opportunity to constrain the related uncertainties, and reveal widespread burning across large regions of western North America during past warm intervals. Whether such episodes also burned large portions of individual landscapes has been difficult to determine, however, because uncertainties with the ages of past fires and limited spatial resolution often prohibit specific estimates of past area burned. Accounting for these challenges in a subalpine landscape in Colorado, we estimated century-scale fire synchroneity across 12 lake-sediment charcoal records spanning the past 2,000 y. The percentage of sites burned only deviated from the historic range of variability during the Medieval Climate Anomaly (MCA) between 1,200 and 850 y B.P., when temperatures were similar to recent decades. Between 1,130 and 1,030 y B.P., 83% (median estimate) of our sites burned when temperatures increased ∼0.5 °C relative to the preceding centuries. Lake-based fire rotation during the MCA decreased to an estimated 120 y, representing a 260% higher rate of burning than during the period of dendroecological sampling (360 to −60 y B.P.). Increased burning, however, did not persist throughout the MCA. Burning declined abruptly before temperatures cooled, indicating possible fuel limitations to continued burning.**

wildfire | climate change | Medieval Climate Anomaly

Ongoing climate change has raised concerns that high temperatures will increase the severity and frequency of wildfires in many regions (1, 2). Since the mid-1980s, warmer springs and summers have increased the frequency and size of fires across the western United States (3, 4). Given the potential for significant turnover in forest composition and biogeochemical responses, such large, infrequent fires could drive substantial changes in subalpine forest landscapes throughout western North America and yield persistent legacies. Large wildfires also have significant impacts on natural resource economies and on humans at the wildland/urban interface. Such impacts motivate efforts to understand the role of anthropogenic climate change in synchronizing fires across large areas (5). Recent large wildfires correlate with more frequent fire weather and climate change, but wildfires are also influenced by human activities and ecological feedbacks (4, 6–9). Untangling how climate changes, ecological feedbacks, and human modifications each contribute to the size and frequency of wildfires is complex but can be constrained, in part, by examining past wildfires and climate change.

For example, when temperatures were similar to today during the Medieval Climate Anomaly (MCA) from *ca.* 1,200–850 y before Common Era (C.E.) 1950 (hereafter B.P.) (10, 11), unusual warmth and drought contributed to increased biomass burning in Alaskan boreal forests and across much of the western United States (12, 13). Here, we evaluate whether the associated warmth also increased the number of sites burned within an individual landscape. If large fractions of individual landscapes burned synchronously at centennial time scales, then ecological turnover and biogeochemical consequences may have been amplified. However, stochastic processes and local effects mediate the link between fire and climate at local scales (14), and more fires at the regional scale of the western United States do not necessarily mean that fires were larger at landscape scales.

Charcoal accumulation in lake sediments provides an opportunity to examine fire frequency in space and time during the MCA and other periods of climate change. When wildfires burn within ∼1–3 km of a lake, a peak in charcoal accumulation within the lake sediment preserves a signal of the fire. Multiple charcoal accumulation records can then be combined to constrain regional changes in biomass burned (13, 15). Charcoal records combined over regional to global scales show that temperature has been a prominent control on biomass burning over millennia and that periods of rapid climate change, including the MCA, have resulted in more biomass burned on large scales (16–18). At landscape scales, however, charcoal records demonstrate the importance of stochastic processes (14, 19, 20).

Furthermore, processes that include sediment mixing, attenuation of charcoal accumulation with distance, vegetation structure and composition, and fire intensity complicate inferring fire size from charcoal accumulation (13, 15, 21). Therefore, we present a new method to evaluate the extent of past fires on landscape scales, which avoids some of these challenges while also incorporating sediment age uncertainty. Our approach estimates the fraction of sample locations burned per century in a single ∼100,000-ha mountain range over the past 2,000 y based on 12 lake-sediment charcoal records. The records provide spatial detail to the fire history of a representative subalpine landscape in Colorado, and yield perspectives on (*i*) variation among stand-scale

## Significance

**In the western United States and other forested regions, climate change may increase both the frequency of wildfires and the amount of area burned. Studies of past climate changes and their effects on wildfires can provide constraints on potential future wildfire risks. Here, we reconstruct the history of wildfire across a representative subalpine forest landscape in northern Colorado over the past two millennia. Warming of ∼0.5 °C ∼1,000 years ago increased the percentage of our study sites burned per century by ∼260% relative to the past ∼400 y. The large increase in the number of sites burned by fires highlights the risk that large portions of individual landscapes may burn as climates continue to warm today.**

Author contributions: W.J.C. and B.N.S. designed research; W.J.C., D.P., C.J.S., G.J.-M., and B.N.S. performed research; W.J.C. and B.N.S. contributed new reagents/analytic tools; W.J.C. and B.N.S. analyzed data; and W.J.C. and B.N.S. wrote the paper.

The authors declare no conflict of interest.

This article is a PNAS Direct Submission.

Data deposition: The data reported in this paper have been deposited in the International Multiproxy Paleofire Database, www.ncdc.noaa.gov/data-access/paleoclimatology-data/datasets/fire-history (accession nos. uselk001, usgem001, usgcr001, usphd001, usphn001, usprb001, usprd001, uspsv001, ussbw001, usptl001, ustig001, and uspwl001).

See Commentary on page 13137.

[1]To whom correspondence should be addressed. Email: wcalder@uwyo.edu.

This article contains supporting information online at www.pnas.org/lookup/suppl/doi:10.1073/pnas.1500796112/-/DCSupplemental.

fire histories, (*ii*) the relationship between climate change and the percentage of sites burned within a landscape, and (*iii*) the comparability of fire regimes during the MCA and recent decades.

After accounting for the age uncertainties of fires detected within the charcoal records (22), we reconstructed the probability that a given number of sites burned within the landscape per century (century-scale synchroneity). The result enables a constraint on the variability of landscape-scale fire regimes over time. The range of estimates reflects our temporal uncertainty, and we focus on periods when significant differences in the percentage of sites burned exceeded the related uncertainty. Because the area around any single lake can burn more than once per century, and thus contribute more than one fire per century to the total, the number of fires in any period could exceed >100% of the number of sites. To compare burning rates in our reconstruction with more recent estimates of fire activity, we used a modified estimate of fire rotation, based on peaks in lake-sediment records. Specifically, we estimated lake-based fire rotation as the time required for $L$ number of fires to be recorded in any number of lakes sampled in the study area, where $L$ is the total number of lakes in our study area. Charcoal accumulation rates normalized to z-scores (deviations for the mean rate measured in SDs) have also been calibrated against area burned (13, 15) and used as an index of biomass burning (12). Here, we compare our analysis of cross-site fire synchrony with the relative measure of past charcoal production rates provided by z-scores.

To conduct our analysis, we collected sediment cores from 12 lakes within and surrounding the Mount Zirkel Wilderness, a mountainous area of subalpine forests in northern Colorado (Fig. 1). Forests across the study region are dominated by *Picea engelmannii* (Engelmann spruce) and *Abies lasiocarpa* (subalpine fir), with *Pinus contorta* var. *latifolia* (lodgepole pine) and *Populus tremuloides* (aspen) more dominant at lower elevations (sites <2,700 m). Two sites, Summit Lake and Seven Lakes, lie near the upper treeline, where the surrounding vegetation consists of bands of spruce-fir forests and open meadows (23), but closed spruce-fir and lodgepole pine forests surround the remaining sites. Fossil pollen data indicate that the regional vegetation remained similar to the regional vegetation observed today throughout the past 2,000 y. Some records show an increase in spruce and fir abundance in the past 500–1,000 y (24–27), and regional timberline changes may be consistent with an expansion of meadows and parklands at the highest elevations (28, 29).

From the 12 charcoal records, we inferred 120 fires over the past 3,000 y and 100 fires between 2,000 and −60 y B.P. (Fig. 2*A*). In

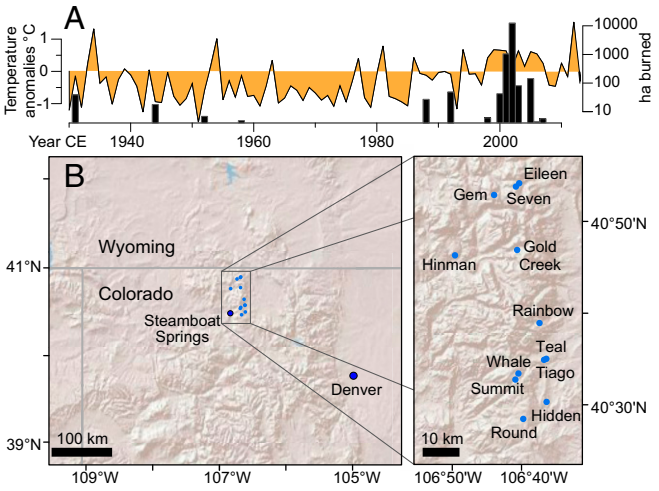


**Fig. 1.** Historic area burned and study area highlighting recent local increased area burned (52). (*A*) Historic area burned and temperature anomalies from our study area show the increased area burned with recent high temperatures. (*B*) Sampling locations of our lake sites within our ∼100,000-ha study area.

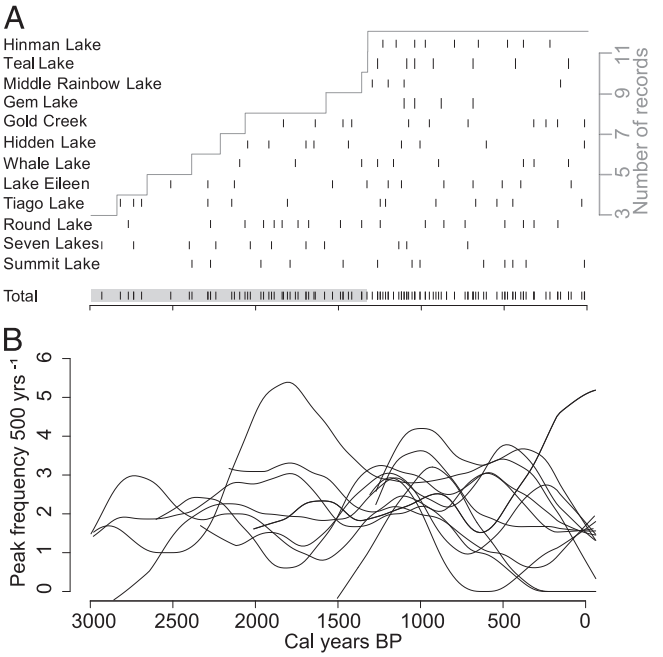


**Fig. 2.** Fire history from our study area shown as individual fires and smoothed fire frequency. (*A*) Tick marks indicate fires recorded by charcoal accumulation at each site, and the gray line marks the length of each record. Note that the diminishing total record is shown in gray. (*B*) Individual fire frequency curves for each site show the wide range of variation at the individual site level, consistent with stochastic influences on fire. Cal, Calculated.

2002, the largest historical fire in our study area, the Mount Zirkel Complex fire, burned 12,648 ha. Only one lake, Gold Creek Lake, falls within the relevant area to have accumulated charcoal from the Mount Zirkel Complex fire (Fig. 1*A*), and consistent with this spatial relationship, Gold Creek Lake has the highest charcoal influx of all lakes in the 21st century (Fig. S1).

Local fire frequency varied among the records, with individual sites deviating from each other in both the direction and magnitude of fire frequency changes over time (Fig. 2*B*). Despite the highly localized changes through time, fire frequency at all sites exceeded more than two fires per 500 y at ∼1,100 y B.P. (Fig. 2*B*).

Both the percentage of sites burned per century and charcoal influx also rose above background levels during the early MCA (Fig. 3). Between 2,000 and 1,300 y B.P., the median and 90% confidence interval (CI) of the percentage of sites burned equaled 50% (90% CI: 31–76%) (Fig. 3*B*). The median for the percentage of sites burned after the MCA was 33% (90% CI: 17–67%). However, during the early MCA between 1,130 and 1,030 y B.P., the median percentage of sites burned increased to 83% (90% CI: 50–108%) (Fig. 3*B*). When the percentage of sites burned peaked between 1,130 and 1,030 y B.P., we estimate ≥95% probability that ≥50% of the sites burned, which indicates a significant deviation from background burning rates. The data also indicate an 8% probability that 100% of the sites burned between 1,130 and 1,030 y B.P., with some potentially burning twice.

To compare burning rates in our reconstruction with other estimates of fire activity, we used a modified estimate of lake-based fire rotation. In the past 420 y, the reconstructed fire rotation derived from dendrochronologies equaled 321 y (30), similar to our median lake-based fire rotation of 315 y (90% CI: 252–387) from 360 to −60 y B.P. During the warm MCA, however, when 83% of our study sites burned, fire rotation fell to 120 y (90% CI: 92–200); the corresponding fire frequency detected between 1,130 and 1,030 y B.P. at the early MCA represents a 260% increase in burning over the past 420 y.

Over the entire record, temperature positively correlated with the median percentage of sites burned ($r$ = 0.55), and a simple linear

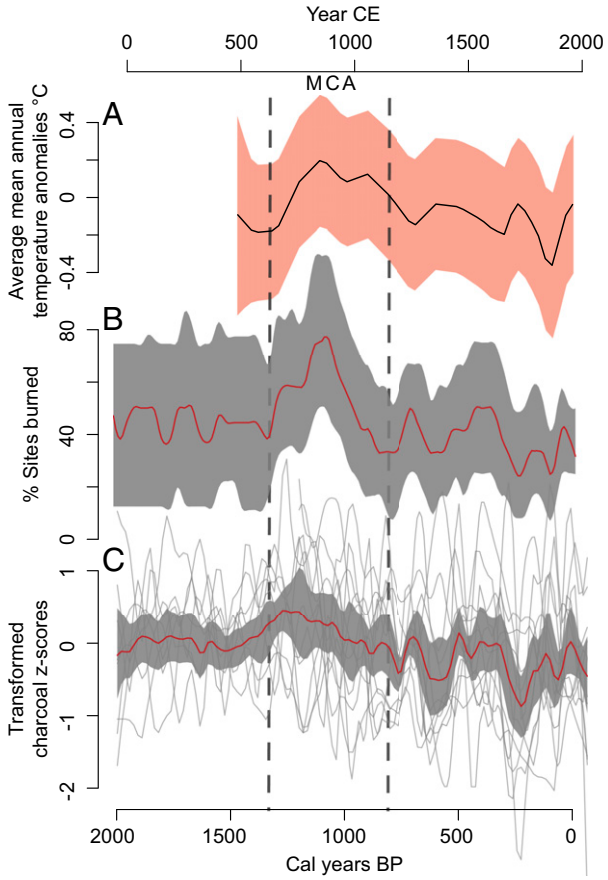


**Fig. 3.** Peak burning and increased charcoal accumulation coincide with maximum temperatures during the MCA. (*A*) Pollen reconstruction of mean annual temperature anomalies for North America calculated using 110-y Lowess smoothing. Anomalies are expressed as deviations from a 1904–1980 North American instrumental average (11). (*B*) Percentage of sites burned per century, with median (red) and 90% CIs (gray band). (*C*) Individual site (gray lines) and combined transformed charcoal z-scores with median (red) and 90% CIs (gray band).

model explains 28.6% of the variance in sites burned per century ($P < 0.01$) (Fig. 4), suggesting an influence of low-frequency temperature trends on the extent of past fires. We considered moisture from regional tree-ring Palmer Drought Severity Index reconstructions (31) in linear and generalized additive models with temperature, but the moisture reconstructions did not improve either model. The relationship of increased temperature and increased fire frequency, however, was not sustained throughout the MCA, and the large fraction of sites burned declined abruptly after 1,080 y B.P. (Figs. 3 and 4).

## Local and Landscape Fire Patterns During Climate Change

Studies at landscape scales in boreal and subalpine forests have argued that multiple lake records from the same area should show synchronous fire episodes if climate exerted a significant influence (14), but there was little to no dependence among Holocene-length fire frequency records (19, 20, 32–34). Consequently, local or stochastic factors, such as topography, vegetation, or lightning strikes, were likely important for influencing fire frequency at individual study sites (14). The highly site-specific fire frequency histories at our sites (Fig. 2*B*) support this inference. Our individual records were, at times, out of phase with each other despite being located on the same landscape, and any one record may or may not directly correlate with centennial-scale temperature trends (Figs. 2*B* and 3*C*).

Within this variability, a high probability exists that the majority of our sites burned in a single century at the beginning of the MCA (Fig. 3*B*), but a high density of records across a large landscape (e.g., ~0.01 lakes per square kilometer across 1,000 km$^2$ in this study) appears to be required to detect such an effect (35). Variation within any individual record often obscures the relationship between climate and fire (Figs. 2*B* and 3*C*), and many study areas may be too small to have burned even during years with extreme fire weather. As records are compared over large study areas, however, the climate signal in the fire history data exceeds the variability found across individual sites and the climatic control on fire becomes apparent. Thus, at regional scales, climate signals can also exceed the background range of stochastic variability (17). Similarly, peak biomass burning during the MCA appeared in data from ~0.01 lakes per square kilometer across 2,000 km$^2$ in Alaska (13), but not in a high-density study (~0.02 lakes per square kilometer) across a small area (200 km$^2$) in Colorado (36). If ideal fire conditions during the early MCA generated even just one large fire complex that burned near many of our sites, the additional charcoal peaks may have produced the significant increase in sites burned, but the rarity of such events even under optimal conditions could mean that such an event, and the attendant increase in charcoal deposition, may not have burned or been detected in a smaller study area in the same region (36). Consequently, both sufficient density and spatial coverage may be needed to detect a significant relationship between stochastically distributed fires and climate at landscape scales.

As the global climate continues to warm, the bottom-up and stochastic influences, such as those influences that generated the local variability in individual lake records, will likely continue to mediate fire responses at landscape scales even as regional-scale fire regimes shift. Consequently, climate change may increase area burned regionally, but stochastic and local processes may result in fires temporarily decreasing or not increasing for decades at any one site (19, 37). Such dynamics, after ~1,080 y B.P., represent one possible explanation for the decline in fire.

## Controls of Large Wildfire Outbreaks

Warming ~0.5 °C at the beginning of the MCA corresponds with the largest increase in the percentage of sites burned (Fig. 3). A mechanism for the increased sites burned could include a

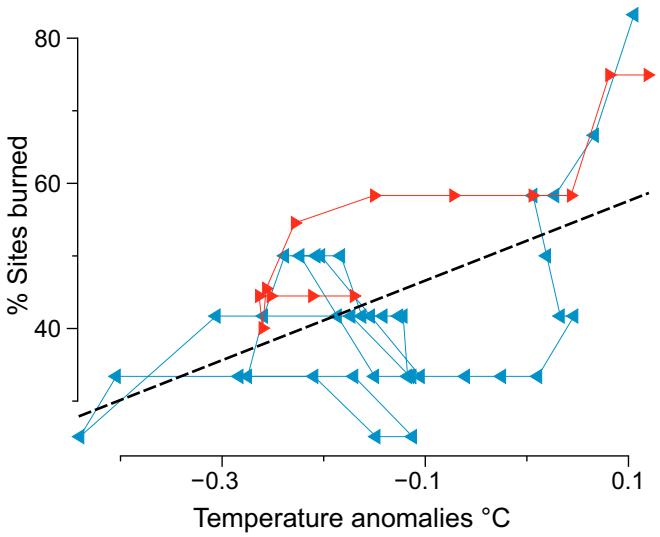


**Fig. 4.** Temperature explains 28.6% of the variance of area burned in a simple linear model (dashed line) ($P < 0.01$ after accounting for temporal autocorrelation). The lines between points are connected through time, with the symbols indicating the general direction of points through time [i.e., the red line generally moves from left (past) to right (toward present), the blue line generally moves from right (past) to left (toward present)]. The different relationship between temperature and the percentage of sites burned when warming (red; 147–1,110 y B.P.) and cooling (blue; 1080–0 y B.P.) indicates a hysteresis between temperature and the percentage of sites burned.

lengthened fire season from warmer temperatures (2, 3). After 1,080 y B.P., the percentage of sites burned decreased abruptly, but because temperatures remained high for another ∼250 y, other factors must explain the subsequent decline in sites burned (Figs. 3 and 4). Moisture changes could explain the decline if moisture changes favored reduced wildfires, but long-term and seasonal moisture trends appear inconsistent with the fire history. In particular, moisture reconstructions from our study region and other portions of the western United States indicate severe drought during the MCA. Reconstructed drought severity increased during or after the percentage of sites burned declined: A regional drought area index achieved its maximum at 1,050–650 y B.P. (38), whereas fire extent declined between 1,080 and 770 BP. The most severe decadal drought in the past 1,200 y in our study region lasted between 804 and 795 y B.P. (39), but overlapped with the period with the lowest median percentage of sites burned between 2,000 and 270 y B.P. Isotopic records from lake sediments in Colorado also indicate increased summer evaporation after ∼1,080 y B.P. (which would favor fire) (40), but the number of sites burned per century declined during this period. Annual and decadal drought trends play an important role in the annual extent of burning (7, 15, 41), but the relationship with aridity appears to differ over long (>100 y) temporal scales (36) and does not explain the decline in the number of fires in our study area.

The absence of a well-documented climatic driver for the abrupt decrease in the percentage of sites burned indicates the potential for hysteresis in the fire-climate relationship, meaning that the relationship of fire to temperature differed depending on direction (warming or cooling), possibly mediated by vegetation or stochastic declines in fire (Fig. 4). Mean charcoal accumulation rates (z-scores in Fig. 3) show a similar pattern as charcoal accumulation also peaked during early MCA warming and declined before temperatures cooled. We hypothesize that hysteresis in the fire-climate relationship could be driven by important vegetation-fire feedbacks or a stochastic decline in fires, which would be relevant to modern climate change impacts (1, 13).

In the first case, multiple vegetation-fire feedbacks potentially contributed to the decline in the number of fires while temperatures were still elevated after ∼1,080 y B.P. For example, young stand ages may alter postfire fuel cover and limit the spread of subsequent fires for the first few decades after a fire. Initially, MCA fires that burned 80% of our study sites would have required new tree regeneration across much of the forest. Such changes in fuel do not typically limit the spread of fire across subalpine forests (despite structural and composition differences among seral stages) (30, 42), but the area burned increases with time since the last fire in spruce-fir–dominated forests (30, 43). Likewise, high-severity fire can burn in young lodgepole stands, but often only under extreme fire weather (42), and old lodgepole stands (>300 y) burn more often and at higher severity than young stands (15, 44). Consequently, the structure of postfire stands during the MCA could have limited the ignition and spread of subsequent fires in the first few decades after the peak in MCA fires.

Legacies of postfire forest structure and regeneration rates that persist over centuries may have further limited fuel accumulation and fire size. Limitations on seed sources (e.g., via burning of nonserotinous coniferous populations) may have increased regeneration time if conditions were unfavorable and large burned patches dominated the landscape (5). Additionally, severe droughts between 1,050 and 650 y BP would have reduced fuel moisture and favored ignition and wildfire spread on scales of days to weeks (45), but droughts after the initial MCA fires may have also reduced postfire germination, killed seedlings susceptible to variations in moisture, and favored the mortality of mature trees either directly or via pathogens. Historically, drought has reduced spruce and fir seedlings and, ultimately, mature tree densities on xeric sites for decades after fire (46). Subalpine forests are typically not considered fuel-limited, but additional analyses could evaluate whether repeated severe droughts over centuries limit fuel connectivity and fire spread through effects on regeneration and mortality.

Finally, stochastic variation in fire could have influenced the decline in fires. Wildfires require multiple factors to burn large portions of the landscape: sufficiently dry fuels, high winds, low humidity, ignition, and sustained severe fire weather from weeks to months. Given the rarity of large fire outbreaks even under optimal climates, the combination of factors required for high-severity fires may simply not have been met during the later portion of the MCA. Each of these hypothesized factors (decreased regeneration and fuels through drought, seed source limitations, and stochastic variation in fire) may have caused or combined to cause fire to decrease while temperatures were still elevated between ∼1,080 and ∼850 y B.P. (Fig. 3).

## Was Burning in the MCA Similar to Today?

Across the western United States, biomass burning increased in the MCA, but regional charcoal production also rose by a similar magnitude at the beginning of the Little Ice Age and with European settlement (12). Our results, however, indicate a significant change in the fraction of landscapes burned during the MCA and at no other period in the 2,000-y record. The large fraction of the landscape burned in and around the Mount Zirkel Wilderness during the MCA has few historic equivalents in the Rocky Mountains. For example, only 15% of our study area burned in the past 80 y (Fig. 1*A*) and only 30% of the area in a 129,600-ha study area in Yellowstone National Park burned from 1890 to 1988 (47). Using Yellowstone National Park fire history as a baseline for comparison, our minimum estimate of 50% of sites burned within a century at the beginning of the MCA exceeds any century-scale estimate of Yellowstone National Park burning for the past 750 y (15, 47).

Comparing past fire regimes with fire regimes of the 20th century involves comparing periods with and without large human modification. However, although humans modified low- to mixed-severity fire regimes in the 20th century, little evidence suggests that human activities caused high-severity fire regimes to exceed the historic range of variability in subalpine forests (7, 48–51). The available evidence suggests that stochastic processes combine with weather and climate to determine the first-order patterns of fire variability at the landscape scale and will continue to be the main drivers for the foreseeable future.

Historically, few landscapes burned as extensively as the Mount Zirkel Wilderness burned during the MCA, but temperatures have only been comparable to the MCA for the past few decades. Within this short period of recent warmth, temperature increases facilitated a substantial rise in area burned even if wildfire has yet to reach the magnitude observed during the MCA (3, 4) (Figs. 1 and 3). Our reconstructed fire-climate relationships show the sensitivity of subalpine systems to increases in mean annual temperature of only ∼0.5 °C and indicate a significant risk that, in the absence of fire-mediated vegetation change and counteracting stochastic declines, fires will burn large areas in the coming century if temperatures continue to rise.

## Materials and Methods

**Study Area and Historic Fires.** In the past 82 y (1930–2012 C.E.), 13,616 ha burned (nonoverlapping) within our study area in the Routt National Forest (Fig. 1). The area burned historically was calculated from class "C" fires or larger (≥4.05 ha) as recorded on archived fire maps and more recent (1985–2012) online fire histories (52). In 2002, the Mount Zirkel Complex fire, the largest fire in our study area since detailed fire maps were maintained staring in the 1930s, burned 12,648 ha (Fig. 1*A*).

To extend the record of area burned through the past 2,000 y, we cored 12 lakes within a sampling area of ∼100,000 ha (Fig. 1*B*). Our sampling area was calculated as a single rectangle that included a 3-km perimeter around each of our coring sites (Fig. 1*B*). However, based on charcoal transport distances (15), charcoal accumulation peaks at these lakes are derived from an area of ∼34,000 ha, which is equivalent to sampling 34% of the landscape. The high density of lakes within the area provides a network of charcoal records near previous fire reconstructions that were developed from dendroecological data (30). Tiago Lake was cored in 1996, and the remaining 11 lakes were cored between 2010 and 2012 (Table S1). All lakes were cored in water deeper than 5 m and were chosen to have similar surface areas (1–6 ha) to limit variation in charcoal records by variations in basin size (Table S1).

**Detecting Past Fires.** Each core was subsampled at 0.5- or 1-cm contiguous intervals. Sediment (1–4 $cm^3$) was sieved at 125 μm and oxidized with household bleach or 6% (wt/wt) hydrogen peroxide (Summit Lake) for 24 h. Charcoal was then counted under a stereomicroscope (with a magnification between 10× and 40×) underlain with a grid pattern to aid counting.

Peaks in charcoal accumulation (pieces of charcoal per square centimeter per year) represent fires in the sampling interval within 1–3 km of the lake and were identified using standard methods in the program CharAnalysis (15, 53). In this paper, we refer to detected peaks as fires for ease of discussion, even though a small probability exists that two or more fires could be combined into a single detected fire event.

In CharAnalysis, charcoal accumulation was first interpolated to the median sampling interval age of all lakes (18 y per subsample; Table S2) as in other multilake charcoal studies (13). Background charcoal was then estimated and subtracted from charcoal accumulation with a Lowess smoother robust to outliers, with a smoothing window chosen based on the best separation of charcoal accumulation peaks from the background (54). Peaks in the residual charcoal accumulation were identified as significant in a two-step process. First, peaks were identified if they exceeded the 99th percentile of the noise distribution in a local Gaussian mixture model. Second, the peaks were screened with a minimum-count test, where significant peaks have <5% chance of being derived from a Poisson distribution of the raw charcoal counts from the previous 75 y (14, 53) (Fig. S1).

**Age Models, Estimating Percentage of Sites Burned, and Fire Rotation.** From the significant peaks identified as fires, we calculated the probability that multiple fires overlapped within 100-y windows to estimate the percentage of sites burned by incorporating the age uncertainties generated from the R package Bchron (22, 55). Bchron models sediment age relationships using a conservative Bayesian framework that constrains sedimentation with the prior information that the sedimentation is monotonic, piecewise linear, and continuous (22). Between calibrated radiocarbon dates (56), ages are randomly selected from the calibrated distributions; sedimentation is then approximated with a random number of break points in a piecewise linear model, following monotonicity and continuity between the two dates. Bchron enables the user to repeat the process thousands of times to generate possible age-sediment models within the prior constraints on sedimentation (Fig. S2). Bchron thus assigns thousands of possible ages to a given depth in a core, which enabled us to generate age probability distributions for the depth of each charcoal peak determined to represent a fire (Fig. S3). For each depth, we generated 20,000 initial ages, removed the first 2,000 (burn-in), and thinned the record by selecting every eighth age for a total of 2,250 possible ages at a given depth.

To estimate century-scale burning as a percentage of sites burned, we used the 2,250 possible ages from 118 of the 120 fires to calculate the frequency that randomly drawn ages for each fire overlapped in a given century. Two of the 120 fires were excluded because the age uncertainty did not extend into the past 2,000 y. Because the number of records decreases further into the past, we constrained our analyses to the past 2,000 y. Because our century-scale window is greater than the sampling interval of sediment, more than one fire from any given lake core could be included in the total sum for each century. The dataset provided 2,250 random combinations of fire ages, which yielded probability distributions (histograms) of the number of fires per century. We used the 5%, 50%, and 95% percentile values from these distributions for the median and 90% CIs of the percentage of sites burned (Fig. 3*B*); the time series was smoothed with a Lowess smoother at a 100-y window.

From the percentage of sites burned, we estimated fire rotation by modifying the equation from Baker (49):

$$FR = \frac{t}{C/L} \quad [1]$$

where *FR* is lake-based fire rotation, *t* is the time window in years, *C* is the total number of charcoal peaks in the given time window, and *L* is the total number of lakes recording. With this modification, Eq. **1** is the inverse of our percentage of sites burned estimate (Fig. 3*B*) for a 100-y time window (49). This approach considers the charcoal source area (a 1- to 3-km radius around a lake that does not change over time) as a point on the landscape and lake-based fire rotation as an estimate of the time required for *L* number of fires to be recorded in any number of sampled lakes. Significant charcoal accumulation peaks represent fire within 1–3 km of a lake (15), but charcoal accumulation peaks do not provide information on how much of the area burned, similar to individual fire-scarred trees in a study plot. If the variation in area burned in a charcoal source were local or stochastic, then the variation over enough time and space would provide an accurate estimate of fire rotation across the landscape. To evaluate this approach, we estimated lake-based fire rotation within the time period (360 to −60 y B.P., 1590–2010 C.E.) that Howe and Baker (30) used to estimate fire rotation from fire scars and stand age reconstructions within a portion of our study area. Their conservative fire rotation estimate (excluding one stand reconstruction that did not preserve evidence of fire) is 321 y.

Our median estimate for lake-based fire rotation across the entire landscape within this same period was similar at 315 y (90% CI: 252–387 y). That is, given the age uncertainty of individual fires, we calculate a median probability of 16 fires from 12 lakes occurring in the past 420 y and an upper 95% and lower 5% probability of 20 and 13 fires, respectively. Howe and Baker's estimate (30) derived from a single watershed of our study area, and variation of fire rotation estimates between watersheds may be different from the entire landscape (48). Regional fire rotation estimates for the past several centuries for subalpine forests in Wyoming and Colorado fall between 225 and 350 y (36, 49), similar to our uncertainty of 252–387 y. The correspondence between our lake-based fire rotation and tree-ring based fire rotation suggests that our assumption of variation in area burned within the charcoal source area is supported by comparisons to spatially and temporally precise fire scar and stand origin fire rotation estimates and represents a close estimate of fire rotation with multiple lake records. As Baker (49) noted, "a list of fires from a small plot. . . can instead be treated as simply point data on fire presence or absence, with fire-regime reconstruction done at the landscape scale." This modification of Eq. **1**, however, remains largely untested as a measure of true fire rotation. We use lake-based fire rotation in this study to provide a common metric for contrasting rates of burning in the past 420 y to the century of peak burning centered at 1,080 y B.P.

Because records with lower temporal resolution affect detection of discrete charcoal accumulation peaks (57, 58), charcoal records from Hinman Lake, Middle Rainbow Lake, and Teal Lake were truncated to the median age of the last calibrated radiocarbon date before sedimentation slowed at these sites at ∼1,300 y B.P. (Fig. S2). Both Hinman Lake and Middle Rainbow Lake records have a significant charcoal accumulation peak (fire) at 1,234 y B.P. (Hinman Lake) and 1,289 y B.P. (Middle Rainbow Lake), close to where the record was truncated. When calculating the percentage of sites burned, these fires at the end of the record proved problematic, because the age uncertainty of the two fires exceeded the end of the calibrated dates. To ensure these fires at the end of the calibrated dates did not inappropriately increase the percentage of sites burned for estimates older than 1,200 y B.P., we resampled the age distributions of the last fire at Hinman Lake and Middle Rainbow Lake from below the 99th percentile of the distribution. Of 2,250 initial possible ages, resampling the age distributions excluded 20 and 23 possible ages from the last fire at Hinman Lake and Middle Rainbow Lake, respectively, and had no meaningful effect on the estimate of the percentage of sites burned. Because these three lake records start near the onset of the MCA, we also tested whether they influenced our results by excluding the three lakes from our percentage of sites burned calculation shown in Fig. 3*B*, and found that they did not alter the results. Excluding the records from Hinman Lake, Middle Rainbow Lake, and Teal Lake generated a similar curve to Fig. 3*B*.

Transformed charcoal z-scores were calculated by rescaling individual charcoal accumulation records in three steps: (*i*) minimax transformation, (*ii*) Box–Cox transformation, and (*iii*) dividing by the SD of the data (59). The records were then smoothed in a two-step process: the samples were first prebinned with nonoverlapping bins to minimize the effects of records with differing resolutions, and they were then smoothed with a Lowess smoother to minimize outliers similar to the methods of Daniau et al. (16) and implemented in the Paleofire R package (60). CIs were calculated by bootstrapping the prebinned charcoal series 1,000 times. We used a bin width of 18 y (same interpolation interval for peak analysis above) and a smoothing window of 100 y (Fig. 3*C*) to keep parameters similar to the time scale associated with our estimates of the percentage of sites burned (Fig. 3*B*).

**Temperature and Area Burned.** Mean annual temperature deviations (30-y averages) were obtained from a recent continental pollen-based temperature reconstruction and used as a representative sample of continental temperature change in the MCA (11) (Fig. 3*A*). The MCA was used as a period of recent warming, but previous periods in the Holocene have been warmer (61). We examined the relationship between temperature and the percentage of sites burned at the same resolution as the temperature data (30-y time steps) using the presmoothed median estimate of the percentage of sites burned in a simple linear model (Fig. 4). Pearson's correlation coefficient was used to evaluate the relationship between temperature and area burned. The effective degrees of freedom were estimated after accounting for first-order temporal autocorrelation in both temperature and the percentage of sites burned (62). The linear model was fit with the lm function in the base statistics R package, and all calculations were performed in R (63).

**ACKNOWLEDGMENTS.** We thank Jeremiah Marsicek, Grace Carter, Devin Houghardy, Danny Vecchio, David Webster, Keith Ingledew, Corianne Calder, Marc Serravezza, Ethan Harris, Ashely Harris, and Aaron Condie for field and laboratory assistance and Mitchell Power, Simon Brewer, and the two reviewers for their helpful comments. National Science Foundation Grant BCS-0845129 (to B.N.S.) supported this project.

1. Westerling AL, Turner MG, Smithwick EAH, Romme WH, Ryan MG (2011) Continued warming could transform Greater Yellowstone fire regimes by mid-21st century. *Proc Natl Acad Sci USA* 108(32):13165–13170.
2. Jolly WM, et al. (2015) Climate-induced variations in global wildfire danger from 1979 to 2013. *Nat Commun* 6(7537):7537.
3. Westerling AL, Hidalgo HG, Cayan DR, Swetnam TW (2006) Warming and earlier spring increase western U.S. forest wildfire activity. *Science* 313(5789):940–943.
4. Dennison PE, Brewer SC, Arnold JD, Moritz MA (2014) Large wildfire trends in the western United States, 1984-2011. *Geophys Res Lett* 41(8):1–6.
5. Turner MG, Baker WL, Peterson CJ, Peet RK (1998) Factors influencing succession: Lessons from large, infrequent natural disturbances. *Ecosystems* 1(6):511–523.
6. Sherriff RL, Platt RV, Veblen TT, Schoennagel TL, Gartner MH (2014) Historical, observed, and modeled wildfire severity in montane forests of the Colorado Front Range. *PLoS One* 9(9):e106971.
7. Morgan P, Heyerdahl EK, Gibson CE (2008) Multi-season climate synchronized forest fires throughout the 20th century, northern Rockies, U.S.A. *Ecology* 89(3):717–728.
8. Aldersley A, Murray SJ, Cornell SE (2011) Global and regional analysis of climate and human drivers of wildfire. *Sci Total Environ* 409(18):3472–3481.
9. Hawbaker TJ, et al. (2013) Human and biophysical influences on fire occurrence in the United States. *Ecol Appl* 23(3):565–582.
10. Mann ME, et al. (2009) Global signatures and dynamical origins of the Little Ice Age and Medieval Climate Anomaly. *Science* 326(5957):1256–1260.
11. Trouet V, et al. (2013) A 1500-year reconstruction of annual mean temperature for temperate North America on decadal-to-multidecadal time scales. *Environ Res Lett* 8(024008):1–10.
12. Marlon JR, et al. (2012) Long-term perspective on wildfires in the western USA. *Proc Natl Acad Sci USA* 109(9):E535–E543.
13. Kelly R, et al. (2013) Recent burning of boreal forests exceeds fire regime limits of the past 10,000 years. *Proc Natl Acad Sci USA* 110(32):13055–13060.
14. Gavin DG, Hu FS, Lertzman K, Corbett P (2006) Weak climatic control of stand-scale fire history during the late holocene. *Ecology* 87(7):1722–1732.
15. Higuera PE, Whitlock C, Gage JA (2011) Linking tree-ring and sediment-charcoal records to reconstruct fire occurrence and area burned in subalpine forests of Yellowstone National Park, USA. *Holocene* 21(2):327–341.
16. Daniau A-L, et al. (2012) Predictability of biomass burning in response to climate changes. *Global Biogeochem Cycles* 26(GB4007):1–12.
17. Marlon JR, et al. (2009) Wildfire responses to abrupt climate change in North America. *Proc Natl Acad Sci USA* 106(8):2519–2524.
18. Power MJ, et al. (2013) Climatic control of the biomass-burning decline in the Americas after AD 1500. *Holocene* 23(1):3–13.
19. Ali AA, Carcaillet C, Bergeron Y (2009) Long-term fire frequency variability in the eastern Canadian boreal forest: The influences of climate vs. local factors. *Glob Chang Biol* 15(5):1230–1241.
20. Barrett CM, Kelly R, Higuera PE, Hu FS (2013) Climatic and land cover influences on the spatiotemporal dynamics of Holocene boreal fire regimes. *Ecology* 94(2):389–402.
21. Ali AA, et al. (2012) Control of the multimillennial wildfire size in boreal North America by spring climatic conditions. *Proc Natl Acad Sci USA* 109(51):20966–20970.
22. Parnell AC, Haslett J, Allen JRM, Buck CE, Huntley B (2008) A flexible approach to assessing synchroneity of past events using Bayesian reconstructions of sedimentation history. *Quat Sci Rev* 27:1872–1885.
23. Hiemstra CA, Liston GE, Reiners WA (2006) Observing, modelling, and validating snow redistribution by wind in a Wyoming upper treeline landscape. *Ecol Modell* 197(1-2): 35–51.
24. Minckley T, Shriver R, Shuman B (2012) Resilience and regime change in a southern Rocky Mountain ecosystem during the past 17000 years. *Ecol Monogr* 82(1):49–68.
25. Minckley TA (2014) Postglacial vegetation history of southeastern Wyoming, U.S.A. *Rocky Mountain Geology* 49(1):61–74.
26. Jimenez-Moreno G, Anderson RS, Atudorei V, Toney JL (2010) A high-resolution record of climate, vegetation, and fire in the mixed conifer forest of northern Colorado, USA. *Geol Soc Am Bull* 123(1-2):240–254.
27. Carter VA, Brunelle A, Minckley TA, Dennison PE, Power MJ (2013) Regionalization of fire regimes in the Central Rocky Mountains, USA. *Quaternary Research* 80(3): 406–416.
28. Fall PL (1997) Timberline fluctuations and late Quaternary paleoclimates in the Southern Rocky Mountains, Colorado. *Geol Soc Am Bull* 109(10):1306–1320.
29. Petersen KL (1994) A warm and wet little climatic optimum and a cold and dry little ice age in the southern Rocky Mountains, U.S.A. *Clim Change* 26(2-3):243–269.
30. Howe E, Baker WL (2003) Landscape heterogeneity and disturbance interactions in a subalpine watershed in northern Colorado, USA. *Ann Assoc Am Geogr* 93(4):797–813.
31. Cook ER, et al. (2008) *North American Summer PDSI Reconstructions, Version 2a*. IGBP PAGES/World Data Center for Paleoclimatology Data Contribution Series 2008-046. Available at www.ncdc.noaa.gov/paleo/pdsi.html. Accessed February 19, 2015.
32. Long CJ, Whitlock C, Bartlein PJ (2007) Holocene vegetation and fire history of the Coast Range, western Oregon, USA. *Holocene* 17(7):917–926.
33. Carcaillet C, et al. (2009) Spatial variability of fire history in subalpine forests: From natural to cultural regimes. *Ecoscience* 16(1):1–12.
34. Hu FS, et al. (2006) How climate and vegetation influence the fire regime of the Alaskan Boreal Biome: The Holocene perspective. *Mitigation and Adaptation Strategies for Global Change* 11(4):829–846.
35. Baker WL (1989) Landscape ecology and nature reserve design in the Boundary Waters Canoe Area, Minnesota. *Ecology* 70(1):23–35.
36. Higuera PE, Briles CE, Whitlock C (2014) Fire-regime complacency and sensitivity to centennial-through millennial-scale climate change in Rocky Mountain subalpine forests, Colorado, USA. *J Ecol* 102(6):1429–1441.
37. Gavin DG, et al. (2007) Forest fire and climate change in western North America: Insights from sediment charcoal records. *Front Ecol Environ* 5(9):499–506.
38. Cook ER, Woodhouse CA, Eakin CM, Meko DM, Stahle DW (2004) Long-term aridity changes in the western United States. *Science* 306(5698):1015–1018.
39. Woodhouse CA, Meko DM, MacDonald GM, Stahle DW, Cook ER (2010) A 1,200-year perspective of 21st century drought in southwestern North America. *Proc Natl Acad Sci USA* 107(50):21283–21288.
40. Anderson L (2012) Rocky Mountain hydroclimate: Holocene variability and the role of insolation, ENSO, and the North American Monsoon. *Glob Planet Change* 92-93: 198–208.
41. Sibold JS, Veblen TT (2006) Relationships of subalpine forest fires in the Colorado Front Range with interannual and multidecadal-scale climatic variation. *J Biogeogr* 33(5):833–842.
42. Renkin RA, Despain DG, Jessie E (1992) Fuel moisture, forest type, and lightning-caused fire in Yellowstone National Park. *Can J Res* 22(1):37–45.
43. Baker WL, Kipfmueller KF (2001) Spatial ecology of pre-Euro-American fires in a Southern Rocky Mountain subalpine forest landscape. *Prof Geogr* 53(2):248–262.
44. Turner MG, Romme WH, Gardner RH (1999) Prefire heterogeneity, fire severity, and early postfire plant reestablishment in subalpine forests of Yellowstone National Park, Wyoming. *International Journal of Wildland Fire* 9(1):21–36.
45. Fauria MM, Michaletz ST, Johnson EA (2011) Predicting climate change effects on wildfires requires linking processes across scales. *Wiley Interdiscip Rev Clim Chang* 2(1):99–112.
46. Peet RK (1981) Forest vegetation of the Colorado Front Range: Composition and dynamics. *Vegetatio* 45(1):3–75.
47. Romme WH, Despain DG (1989) Historical perspective on the Yellowstone fires of 1988. *Bioscience* 39(10):695–699.
48. Sibold JS, Veblen TT, Gonzalez ME, Park MN (2006) Spatial and temporal variation in historic fire regimes in subalpine forests across the Colorado Front Range in Rocky Mountain National Park, Colorado, USA. *J Biogeogr* 33(4):631–647.
49. Baker W (2009) *Fire Ecology in Rocky Mountain Landscapes* (Island Press, Washington, DC).
50. Moritz M, Parisien M, Batllori E (2012) Climate change and disruptions to global fire activity. *Ecosphere* 3(6):1–22.
51. Schoennagel T, Veblen TT, Romme WH (2004) The interaction of fire, fuels, and climate across Rocky Mountain forests. *Bioscience* 54(7):661–676.
52. Geosciences and Environmental Change Science Center (2014) Federal wildland fire occurrence. Available at wildfire.cr.usgs.gov. Accessed February 26, 2014.
53. Higuera PE, Brubaker LB, Anderson PM, Hu FS, Brown TA (2009) Vegetation mediated the impacts of postglacial climate change on fire regimes in the south-central Brooks Range, Alaska. *Ecol Monogr* 79(2):201–219.
54. Kelly RF, Higuera PE, Barrett CM, Hu FS (2011) A signal-to-noise index to quantify the potential for peak detection in sediment–charcoal records. *Quaternary Research* 75(1):11–17.
55. Haslett J, Parnell A (2008) A simple monotone process with application to radiocarbon-dated depth chronologies. *J R Stat Soc Ser C* 57(4):399–418.
56. Reimer P, et al. (2013) IntCal13 AND Marine13 Radiocarbon age calibration curves 0–50,000 years cal BP. *Radiocarbon* 55(4):1869–1887.
57. Carcaillet C, et al. (2001) Change of fire frequency in the eastern Canadian boreal forests during the Holocene: Does vegetation composition or climate trigger the fire regime? *J Ecol* 89(6):930–946.
58. Higuera PE, Gavin DG, Bartlein PJ, Hallett DJ (2010) Peak detection in sediment–charcoal records: Impacts of alternative data analysis methods on fire-history interpretations. *International Journal of Wildland Fire* 19(8):996–1014.
59. Power MJ, et al. (2008) Changes in fire regimes since the Last Glacial Maximum: An assessment based on a global synthesis and analysis of charcoal data. *Clim Dyn* 30(7): 887–907.
60. Blarquez O, et al. (2014) Paleofire: An R package to analyse sedimentary charcoal records from the Global Charcoal Database to reconstruct past biomass burning. *Comput Geosci* 72:255–261.
61. Shuman B (2012) Recent Wyoming temperature trends, their drivers, and impacts in a 14,000-year context. *Clim Change* 112(2):429–447.
62. Dawdy DR, Matalas NC (1964) Statistical and probability analysis of hydrologic data, Part III: Analysis of variance, covariance and time series. *Handbook of Applied Hydrology, a Compendium of Water-Resources Technology* (MacGraw–Hill Book Company, New York), pp 8.68–8.90.
63. R Development Core Team (2014) *R: A Language Environment for Statistical Computing* (R Foundation for Statistical Computing, Vienna, Austria).